Time-Decorrelated Multifocal Micromachining and Trapping

David N. Fittinghoff, Chris B. Schaffer, Eric Mazur, and J. A. Squier

***Abstract*—Temporally decorrelated multifocal arrays eliminate spatial interference between adjacent foci and allow multifocal imaging with the diffraction-limited resolution of a single focus, even for foci spaced by less than the focal diameter. In this paper, we demonstrate a high-efficiency cascaded-beamsplitter array for producing temporally decorrelated beamlets. These beamlets are used to produce a multifocal microscope with which we have demonstrated two-photon fluorescence imaging, multifocal micromachining of optical waveguides, and multifocal optical trapping.**

***Index Terms*—Micromachining, multifocal microscopy, multiphoton microscopy, optical tweezers.**

I. Introduction

MULTIFOCAL microscopes allow the efficient use of the energy from the ultrashort-pulse lasers that are currently used for multiphoton microscopy [1]–[3]. By distributing the laser power over many foci, these microscopes use more of the available laser power while keeping the power in each beam below the damage threshold for the sample being studied. One difficulty that arose in early multifocal microscopes, however, was interference between the overlapping tails of adjacent foci, which reduces the resolution of the microscope as the foci are moved closer together [1], [2]. To avoid this difficulty, temporally decorrelated multifocal microscopes introduce a different delay in the pulse arrival time of each focus [4]–[6]. Since the pulses in each beamlet do not overlap in time, the interference is eliminated, and the foci may be placed arbitrarily close together without degradation of the resolution of the microscope.

In addition to increasing the efficiency for multiphoton imaging, temporally decorrelated multifocal microscopes can also have a profound effect on micromachining and trapping. In micromachining with ultrashort-pulsed lasers, one limitation has been the need to machine a single point at a time. By using a temporally decorrelated array, one can conceivably arrange a large number of foci to cover a planar area and machine the entire area simultaneously. Even more promising is the potential to control each focus individually using a micromirror array or optical modulator to machine, in parallel, a large arbitrarily shaped device with a feature size set by the resolution of a single focus. A similar temporally decorrelated array could also be used as parallel optical tweezers to trap particles in any two-dimensional pattern desired.

In this paper, we discuss the design of our most recent temporally decorrelated microscope, including the scaling of the optical efficiency with number of foci, how to produce decorrelated beamlets that contain all of the available laser power, the means of producing multiple foci from the beamlets, and the alignment and resolution of the resulting microscope. We then demonstrate multifocal machining and trapping and discuss means of expanding the capability of each technique.

Manuscript received February 23, 2001; revised August 10, 2001. This work was supported in part by the National Science Foundation under Grant DBI-9987257.

D. N. Fittinghoff is with the Institute for Nonlinear Science, University of California at San Diego, La Jolla, CA 92093-0339 USA (e-mail: dfittinghoff@ucsd.edu).

C. B. Schaffer is with the Department of Physics, Harvard University, Cambridge, MA 02138 USA (e-mail: schaffer@physics.harvard.edu).

E. Mazur is with the Department of Physics and the Division of Engineering and Applied Sciences, Harvard University, Cambridge, MA 02138 USA (e-mail: mazur@physics.harvard.edu).

J. A. Squier is with the Electrical Engineering and Computer Science Department, University of California at San Diego, La Jolla, CA 92093-0339 USA (e-mail: jsquier@ycsd.edu).

Publisher Item Identifier S 1077-260X(01)09940-3.

II. Temporally Decorrelated, Multifocal, Multiphoton Microscopy

One means of increasing the efficiency (and potentially increasing the image acquisition speed) in multiphoton microscopy is to distribute the laser power over many foci and scan all the foci instead of scanning only one focus. This method uses more of the available laser power while keeping the power in each beam below the damage threshold for the sample being studied.

A. Scaling With Number of Foci and Laser Power

The cell viability data of König *et al.* [7] indicated a loss of cell viability of Chinese hamster ovary cells under exposure to 70-pJ 150-fs 800-nm pulses at 80-MHz repetition rate. Assuming that the damage limitations are associated with the peak power of each focus, there is a large potential increase in the excitation efficiency by using more of the available laser energy by distributing the laser power over multiple foci. Consider an extended-cavity Ti : Sapphire oscillator with a 22-MHz repetition rate that is capable of producing 20-nJ 20-fs pulses. Dividing this energy among 64 foci and scaling for pulsewidth and other parameters, there is a potential improvement in the efficiency of excitation of more than two orders of magnitude over the efficiency of a single focus. While different damage mechanisms may introduce other limitations, the potential increase in efficiency makes using multiple foci attractive.

B. Temporally Decorrelated Beamlet Arrays

A common method of producing multiple foci in multiphoton microscopes relies on placing a microlens array in the beam

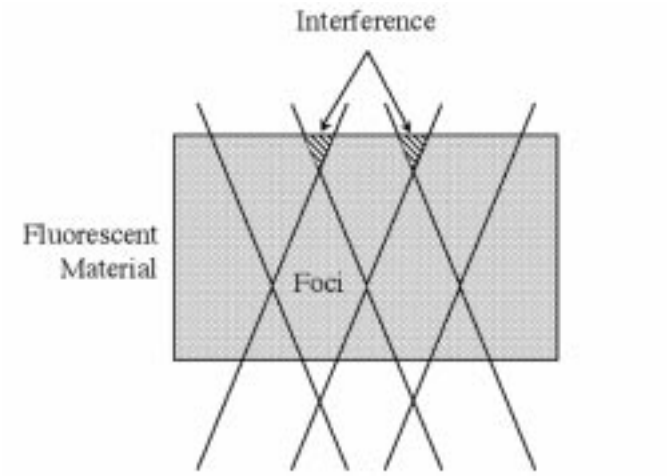

Fig. 1. The out-of-focus tails of multiple beams focusing in a fluorescent material can interfere inside the material.

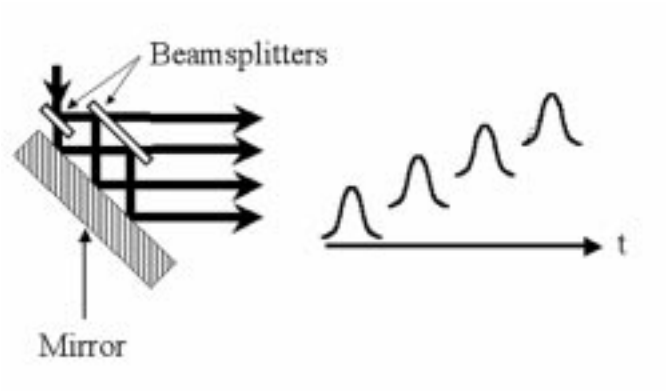

Fig. 2. High-efficiency cascade of beamsplitters combined with a mirror for producing a temporally decorrelated beamlet array.

to produce a series of beamlets [1]–[3]. These beamlets are then appropriately relayed to the entrance pupil of the objective and scanned with galvanometric scanners [2] or with a rotating lenslet array [1]. The multiphoton fluorescence signal is then imaged to a charge-coupled device array. A limitation of this method is that as the foci are placed closer together, interference between the overlapping, out-of-focus tails of adjacent beamlets can generate significant multiphoton signal. Fig. 1 shows schematically how the beams can overlap outside the focal plane. For wavelengths near 800 nm and numerical apertures (NAs) near 1.3, this effect greatly degrades the contrast for separations of less than $\sim$7–10 μm between the foci [2], [6]. Because ultrashort laser pulses ($<$1 ps) are often used for multiphoton imaging, the interference between the out-of-focus tails of the pulses can be eliminated or reduced if the pulses arrive at different times, a method first suggested by Buist *et al.* [2].

In [4] and [5], we described two methods of producing an array of beamlets with a time delay between subsequent beamlets, which can then be used to build a temporally decorrelated multifocal microscope. We now use a third, simpler, and more efficient method, but all three methods rely on creating an optical path difference between beamlets that are parallel. The beamlets must be parallel so they can be properly relayed to the entrance aperture of the microscope objective. The first method relies on the propagation of the beamlets through different lengths of material. In this method, the delay difference between any two beams is just

$$\Delta\tau = \frac{\Delta L}{c}(n-1) \tag{1}$$

where the index of refraction of air is set to one and

ΔL difference in material thickness for the two beams;
n index of refraction of the material;
c speed of light in vacuum.

Consider a 20-fs pulse in a glass with a refractive index of 1.5; then producing a temporal separation of twice the pulse width requires only $\Delta L \approx 24$ μm. Thus it is possible to produce a simple optical mask to introduce the delays. A variation of this idea has already been used to produce beamlets from a larger beam. An optical mask of varying thickness was used to produce beamlets for a rotating microlens-based multifocal microscope [6]. Using diffraction theory, Egner *et al.* also showed the theoretical advantage of decorrelating the pulses. While this method works well for the rotating microlens array, any diffraction at the edges between areas of the masks has the potential to degrade the focusing of the beamlets and the resolution of the microscope.

A second method for temporally decorrelating the beamlets, which does not have the limitation due to beamlet diffraction discussed above, is to use an etalon to produce the beamlets [4]. In this method, the path difference taken by different beamlets produced by the etalon produces the temporal decorrelation. This method has the advantage that, except for short propagation distances in air and the dispersion of the mirrors, the pulses in all beamlets experience the same dispersion. For an etalon at 45° with respect to the input beam, with an output beamlet separation of S, the optical delay difference between successive beamlets is given simply by

$$\Delta\tau = \frac{2S}{c}. \tag{2}$$

Because the minimum separation is set by the input beam width at the entrance to the etalon, which is typically at least a couple of millimeters, the delays produced are typically on the order of 10 ps or more. These delays are more than sufficient for the majority of pulses used for multiphoton imaging. The etalon, however, has an optical efficiency of only a few percent because high-reflectivity mirrors are needed to produce nearly equal powers in the beamlets. While it is theoretically possible to design etalons with variable reflectivity to produce uniform beamlets, such an etalon would be expensive to produce and would require a different design if the number of beams or the spacing between the beamlets is changed. Moreover, virtually any design would be at best 50%–60% efficient. To image or machine a large area with the most efficient use of the laser source, it is desirable to produce a temporally decorrelated array that uses all of the incident laser light.

Fig. 2 shows the new high-efficiency beamlet array design we currently prefer. It is based on cascaded 50/50 beamsplitters and one highly reflective mirror. By first dividing the power into two equal beams, then into four beams, eight beams, and so on, we can produce rows of 2^{N} beamlets, where N is the number of

cascaded beamsplitters. We can achieve a two-dimensional temporally decorrelated array of size $2^{\mathrm{N}} \times 2^{\mathrm{M}}$, simply by placing M beamsplitters and a second mirror to operate on the entire row of 2^{N} beamlets in the plane orthogonal to the plane of the initial row of beamlets. This cascade design is simple and relatively compact. Moreover, it does not require custom optics and is extremely efficient since all the incident energy is used. As long as the beamlets are evenly spaced, the successively increasing delays through the cascaded beamsplitters are approximately the same as for the etalon-based method and produce temporal delays on the order of 10 ps or more between the beamlets. One difference is that different beamlets do propagate through different numbers of beamsplitters. Thus, pulses in different beamlets can pass through different amounts of material. If thin beamsplitters are used, the effect on the pulse width due to dispersion can be minimized, but use of extremely short pulses will limit the number of beamlets that can be used without producing different pulse widths in the beamlets.

The real limitations on how close together the beams may be placed are set by the clear aperture required by the input beam, the thickness of the beamsplitter, and how close to its edge the beamsplitter is coated. The problem of choosing the proper clear aperture is similar to that of choosing the "clip width" in a knife-edge measurement of a laser beam [8], where the width chosen depends on the mode or modes of the laser beam. Because the beamlets are imaged to the entrance aperture of the objective with a large magnification, their shape is strongly dependent on the clipping, and we take care that they are not visibly clipped when imaged to the entrance aperture.

C. Imaging the Beams to the Objective

Once we have produced the temporally decorrelated beamlet array, we must transform those beamlets into separate foci in the sample. We achieve this goal using the system shown in Fig. 3. First, we focus the beamlets. At that focus, the beamlets have infinite radius of curvature but different angles of incidence. A pair of lenses then acts as a telescope to image from that focal plane to the entrance aperture of the objective with magnification. The combination of this focus and telescope accomplishes three major tasks.

1) Because the beamlets have different incidence angles at the focus, they also have different incidence angles at the entrance aperture of the objective.
2) Because the beamlets have infinite radius of curvature at the focus, they are collimated and have infinite radius of curvature at the entrance aperture of the objective.
3) By choosing the lenses in the telescope to give an appropriate magnification of the focused spot, we can also properly fill the entrance aperture of the objective.

An infinity-corrected objective then produces an array of foci from these incident beamlets. A linear array of equal intensity, evenly spaced beamlets is transformed into a line of equal intensity, evenly spaced foci. Likewise, a rectangular array of beamlets is transformed into a rectangular array of foci.

As shown in Fig. 3, we also insert a pair of scanning mirrors into the system. This allows us to scan the entire array of foci within the sample. We note that the intensity of the focused beamlets on the first mirror M1 must be below the damage threshold of the mirror. Finally, by inserting a detection arm with a dichroic mirror, tube lens, and camera, we can perform multifocal multiphoton fluorescence imaging with the resolution of single-point illumination.

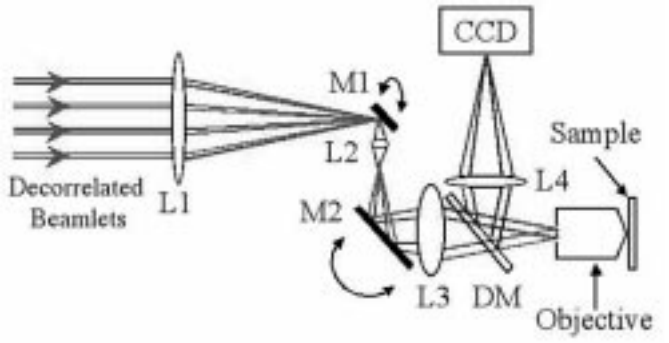

Fig. 3. System to image the decorrelated beamlets to the entrance aperture of the objective. At the focus of lens L1, all beamlets focus and have infinite radius of curvature. Lenses L2 and L3 then act as a telescope to image that focal plane to the entrance aperture of the objective. M1 and M2 are scanning mirrors. DM is a dichroic mirror to separate the fluorescence signal from the incident beam and L4 is the tube lens for the objective. For clarity, only four beamlets are shown initially incident, and only two beamlets are shown after mirror M1.

While the problem of focusing the off-axis beamlets is nonparaxial, we can easily determine the approximate characteristics of the beams by considering the paraxial propagation of an on-axis Gaussian beamlet from lens L1 to the entrance aperture of the objective. In this simple approximation [9], a beamlet, at wavelength λ, incident on the lens L_1 will focus at a distance d

$$d = \frac{f_1}{1 + f_1^2/z_0^2} \tag{3}$$

from the lens. Here $z_0 = \pi w_0^2/\lambda$ is the Rayleigh range of the input beamlet. The $1/\mathrm{e}^2$ radius at the focus is then

$$w_1 = \frac{\lambda f_1}{\pi w_0} \frac{1}{\sqrt{1 + f_1^2/z_0^2}}. \tag{4}$$

At the focus, the beamlets overlap and have infinite radii of curvature. The next step then is to image the beamlets from this focus to the entrance aperture of the objective. At the entrance aperture, all the beams must be collimated and overlapping (centered on the aperture), and they must have the appropriate beam waist to fill the entrance aperture. We use two lenses for this imaging: L2 and L3 in Fig. 3. The exact spacing of the lenses and sizes of the beams should be ray-traced to properly take into account the diffraction of the beamlets. In our initial experiments, lens L1 has a focal length of ~400 mm, so an incident beamlet with ~1-mm diameter focuses to a ~190-μm focal radius at a distance of ~340 mm from the lens. L3 is the Zeiss tube lens for the Zeiss objective and has a focal length of 164 mm. To achieve the smallest spot size at the focus of the microscope objective, the distance from the tube lens to the entrance aperture of the objective should be close to the ~100-mm tube length the objective is designed around.

For a given focal length of L1, the size of the entrance aperture of the objective then determines the focal length required for L2. The entrance aperture of the Zeiss 100 ×/1.25 NA Achroplan in-

finity-corrected objective that we use is ∼5 mm in diameter. We chose a 16-mm achromat for L2 and calculated that the beam at the entrance to the objective should be ∼4 mm in diameter for a 1-mm input beamlet diameter, which would have underfilled the objective slightly. We found, in practice, that we could produce input beams slightly under 1 mm, which increased w_1 and allowed us to just fill the entrance pupil of the objective.

We chose L1 to have as long a focal length as could reasonably be used on our optics table. This increases the size of w_1 (which allows L2 to have a longer focal length, and therefore to be easier to align) without decreasing the input beam diameter, which was kept as large as possible to reduce nonlinear effects in the optical system. Once the beam is split into beamlets, the risk of unwanted nonlinear effects in the optical system decreases except in L2, where the size of each beamlet is quite small, and on M1, where the beamlets are focused. In practice, we were able to avoid unwanted nonlinear effects or damage because the powers required for imaging or machining at an NA of 1.25 are low.

The actual alignment of the imaging is simple in practice once the rough positions of the lenses are known. First, we check that the beamlets are collimated and that they are parallel over a distance of about 4 m. Second, we insert L1 and focus the beamlets onto M1. Third, we adjust the tilt of M1 so that the beams are still parallel to the table and insert L2 at the calculated distance. Fourth, we insert L3 at the calculated distance, adjusting its position to collimate the beamlets. Fifth, we turn on the scanning for M1 and adjust the position of L2 until the beamlets no longer move at the position of the entrance aperture to the objective. Because of the high magnification of L2 and L3, the position of L2 is extremely sensitive, so we mounted it on a micrometer driven translation stage. The position of the foci on M1 relative to the scan axis is also extremely sensitive, so the position of M1 is also adjustable with a micrometer. At this point, it may be necessary to recollimate the beamlets at the entrance aperture position by adjusting the position of L3. A few iterations of these adjustments should produce series of collimated beamlets at the entrance aperture. If the beamlets are not all centered on the same spot, it is probable that they are not parallel when they enter L1. Minor adjustments of the beamlet array may be necessary to overlap the beamlets at the entrance to the objective. We then insert the objective, dichroic mirror, and camera and use two-photon fluorescence from a cell containing coumarin dye to focus the detection. At this point, there should be multiple foci in the dye cell. If foci are missing or are weaker than others, we adjust the beamlet array to maximize and equalize the intensity of the foci.

D. Temporally Decorrelated, Multifocal, Multiphoton Imaging

Fig. 4 shows a two-photon fluorescence image in a coumarin dye cell made using an 8×2 array of temporally decorrelated foci produced by the cascaded beamsplitter technique described above. We used a ∼800-nm extended-cavity Ti : Sapphire oscillator running at a repetition rate of 22 MHz. The difference in intensity between the two rows is due to a beamsplitter that is not exactly 50/50. With a 50/50 beamsplitter, all the foci can have equal intensity.

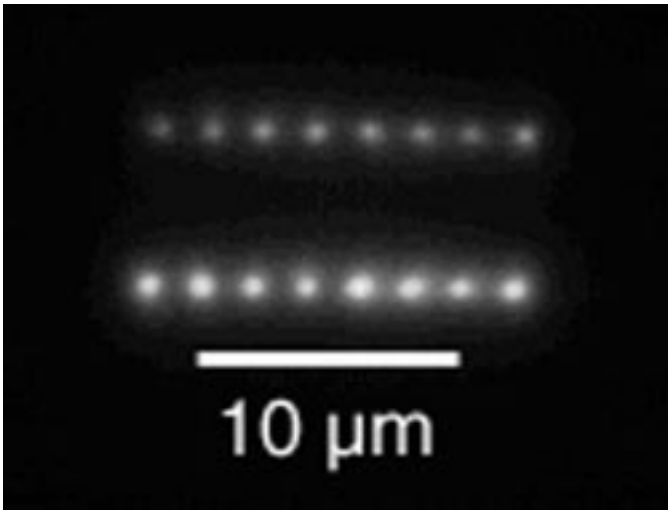

Fig. 4. Two-photon fluorescence from an array of foci produced in coumarin dye using a temporally decorrelated multifocal microscope. The measured axial point spread function for all 16 beams is 1.5 μm.

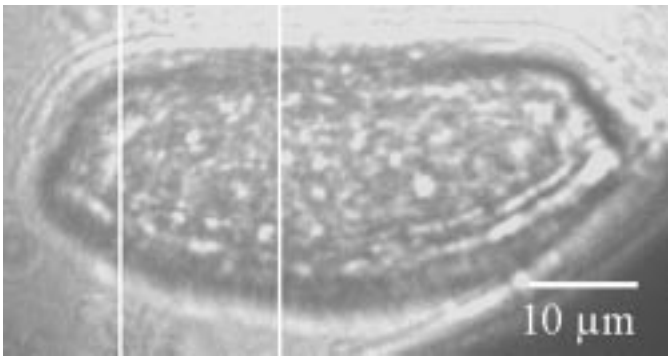

Fig. 5. Brightfield image of a pollen grain from *Clivia Mineata*. The area between the two vertical white lines is the region scanned to produce the 3-D rendered image in Fig. 6.

The resolution of a microscope is set by the point-spread function (PSF), which is the optical response of the system to a point object. A measure of the axial PSF, which is the optical response along the axial dimension, may be obtained by axially scanning an interface between a coverslip and a two-photon-fluorescent dye through the focus. From plane-wave diffraction theory, the axial resolution is then approximately the 17%–83% risetime of the total emitted two-photon fluorescence signal.

We measure an axial PSF with a 17%–83% risetime of ∼1.5 μm for the 16 foci array, which is near the theoretical resolution for the objective for a single beam. Without temporal decorrelation, the PSF would be significantly larger due to the spatial interference between adjacent beamlets. Using this 8×2 array, we imaged by asynchronously rastering the scanning mirrors to fill in the gaps between the foci. As an example of the sectioning capability of the multifocal microscope, we took a stack of two-photon absorption autofluorescence images of a section through a grain of pollen from Clivia Mineata, which is shown in a brightfield image in Fig. 5. We took 46 sections with an exposure time of 2 s for each image. The axial spacing between the sections was 0.5 μm, and the region covered in the stack is shown in Fig. 5. The objective used was a Zeiss 100×/1.25-NA

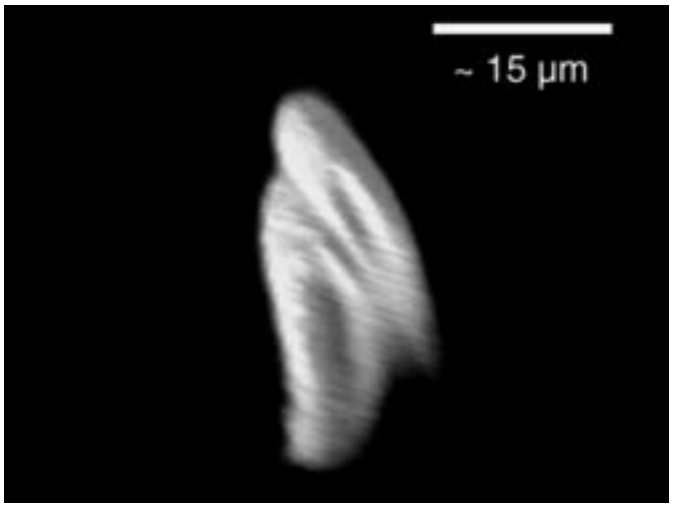

Fig. 6. Three-dimensional rendering of a slice through the grain of pollen shown in Fig. 5. The image is produced from 46 sections spaced by 0.5 μm in the axial direction that were taken in using two-photon autofluorescence with the temporally decorrelated multifocal microscope. This is a side view of the rendering.

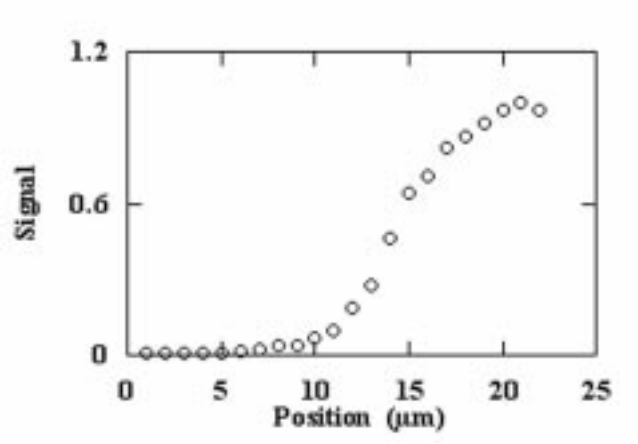

Fig. 7. Measurement of the point spread function using eight decorrelated foci. The laser used is a 1-kHz Ti : sapphire regenerative amplifier. The focusing objective is a Zeiss 100×/1.25 NA Achroplan.

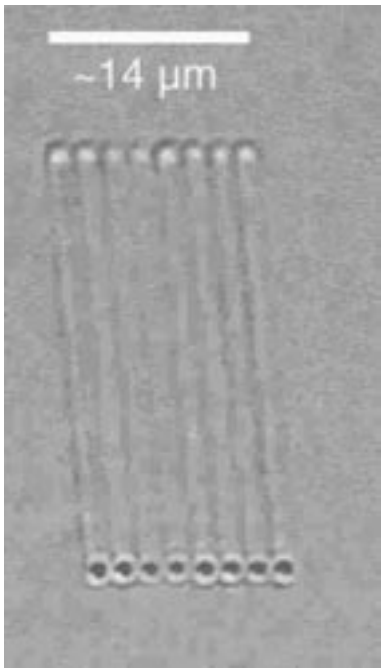

Fig. 8. Set of eight lines written simultaneously in a glass slide using the temporally decorrelated microscope. Eight foci were used and the sample was scanned to produce the lines.

Achroplan oil objective. The total average power in all 16 beamlets was 200 mW, measured in front of the objective. The average power per beam is comparable to the average power that is typically used in two-photon fluorescence imaging. Fig. 6 shows a three-dimensional rendering of the image stack. The autofluorescence is confined largely to two sac-like internal membranes, one of which rests on top of the other. The green autofluorescence is most likely from flavins, which are known to be concentrated in internal membranes of pollen [10]. The clear separation of the membranes, which are only $\sim$1.5 μm thick in the image, shows the high-resolution sectioning ability of the multifocal microscope. We note that other than thresholding for the 3-D rendering in Fig. 6, all the images in this paper are raw data without image processing or sampling.

III. Multifocal Micromachining

In addition to imaging, the temporally decorrelated multifocal array also offers an advantage to multifocal machining with ultrashort pulse lasers. In ultrashort pulse machining, it can be difficult to write structures quickly because of the frequently low repetition rates of the amplified laser systems used for machining. Using multiple foci can reduce the writing time by a factor equal to the number of foci used for the machining. While a multifocal microscope based on a spinning or rastered lenslet array could machine an area, it is not suited to writing an arrangement of small structures close together. The temporally decorrelated multifocal microscope based on the beamsplitter design in Fig. 2, however, can write with all foci simultaneously even with the foci very close together. Moreover, it would be simple to address each focus individually using a multimirror array or optical modulator. By placing foci close together or, using polarization multiplexing [6], overlapping them, it would then be possible to machine an area while turning the power on or off in individual foci to produce complex structures.

While we have not yet demonstrated individual control of the beams, we have used our temporally decorrelated multifocal microscope to address the problem of writing multiple parallel structures in glass. When written at low enough powers and scan rates, lines of damage written in glasses have been shown to act as waveguides [11]–[14]. We used a Ti : Sapphire regenerative amplifier producing $\sim$30-fs pulses at 1.17 kHz repetition rate. Fig. 7 shows a measurement of the axial PSF using this laser and the Zeiss 100×/1.25 NA objective with eight foci. The axial PSF is $\sim$5 μm long. Unlike the result using the oscillator, for which a measurement is given in [4]–[6], the resolution of this setup is not at the diffraction limit for the 1.25 NA objective. In this case, the beam quality of the regenerative amplifier, combined with a slight underfilling of the input aperture of the objective, prevents such resolution. Fig. 8 shows a set of parallel lines machined inside a borosilicate glass slide using these eight foci. The average power used for the machining was 0.53 mW in all

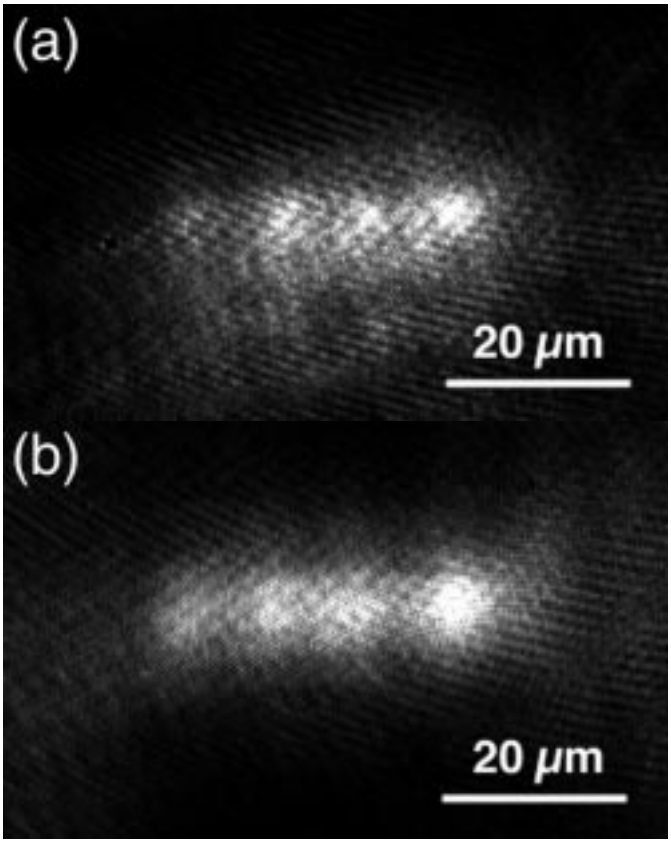

Fig. 9. Images of the near-field output mode of the waveguides. One can clearly see four distinct outputs. The waveguide that extends all the way through the sample into which light was coupled is on the right in the image. (b) Shows the near-field output mode of four waveguides written all the way through the fused silica piece using 2 μJ per beamlet and translating the sample at 20 μm/s. Light was again coupled into the waveguide on the right.

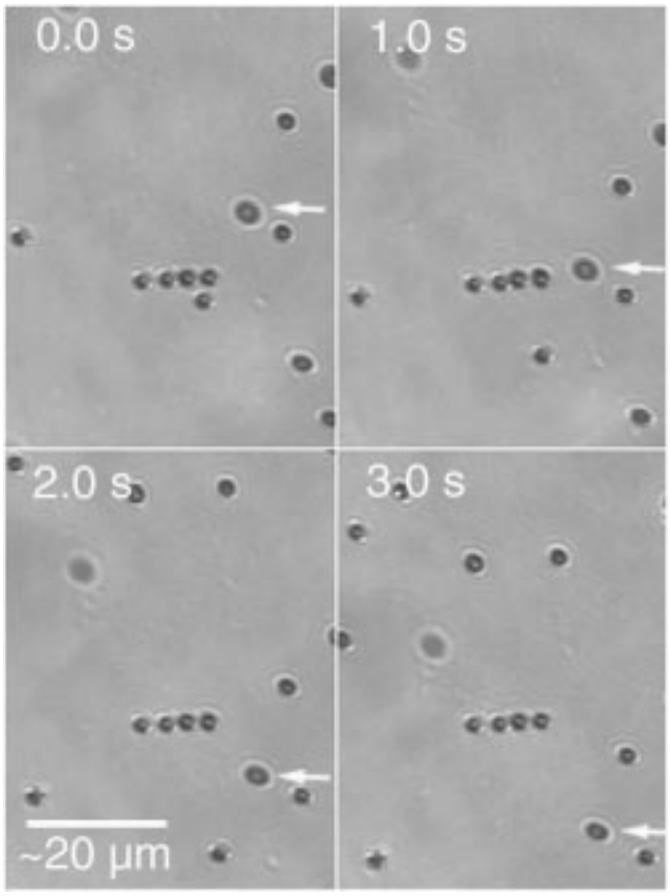

Fig. 10. A montage of frames from a brightfield movie of 2-μm beads being held in the foci as the sample is translated at 10 μm/s. The time between each successive frame is 1.0 s, as is indicated on the montage. One bead is held in each of four foci near the center of the frame as the other beads flow down with respect to the images. To highlight the motion of the other beads, we have used a white arrow in each frame to indicate the position of one of the flowing beads. The objective was a 40×/0.65 NA Zeiss Achroplan oil objective.

eight beams. Since the transmission of the objective is ~60%, the energy per pulse is ~50 nJ, or about ten times the threshold in the material for this focusing [14]. The sample was scanned at 10 μm/s perpendicular to the incident direction of the laser beam to produce the lines and required less than 3 s to write.

A more important demonstration is to write structures such a waveguides or waveguide couplers by translation along the axial dimension of the beam. For this work, we need a long working distance combined with closely spaced foci. Thus, we used a ~0.1 NA, 10× aspheric lens and the beamsplitter array to produce four foci spaced by 10 μm. The axial PSF of the array was measured to be ~90 μm at the top and bottom of a 1-cm-thick piece of fused silica, indicating that the focal properties for this low NA system were not greatly affected by propagation of the focusing beamlets through excess material. Using 1 μJ per beamlet, we machined sets of parallel waveguides by translating the 1-cm fused silica plate axially through the focus. The translation speed was 10 μm/s. We began machining with four beams and successively blocked beams during the machining process so that the number of waveguides goes from four to three to two to one inside the sample, with only one waveguide extended all the way through the sample. To show that this structure acts as a waveguide coupler, we have polished the ends of the plate to remove pitting at the surface and coupled light from a He : Ne laser into the single waveguide end of the structure. Fig. 9(a) shows an image of the near-field output mode of the waveguides. One can clearly see four distinct outputs. The waveguide that extends all the way through the sample into which light was coupled is on the right in the image. Fig. 9(b) shows the near-field output mode of four waveguides written all the way through the fused silica piece using 2 μJ per beamlet and translating the sample at 20 μm/s. Light was again coupled into the waveguide on the right.

While the examples in this paper use a low-repetition-rate regenerative amplifier that is not well suited to rapid micromachining, new extended-cavity Ti : Sapphire oscillators have pulse energies up to 100 nJ at repetition rates of ~15 MHz [15]. With a modest improvement in power from the oscillator, cavity dumping, or two stages of continuous-wave amplification, these oscillators could be used for much more rapid micromachining with multiple foci.

IV. Multifocal Trapping

Another problem for which the multifocal microscope may prove to be useful is that of optically trapping multiple objects, although temporal decorrelation is not strictly necessary. An optical trap uses the forces generated on an object near the focus

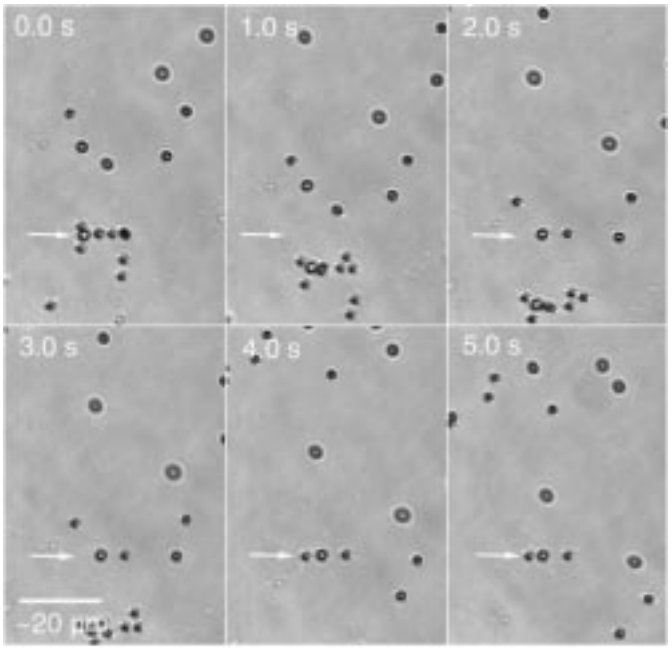

Fig. 11. A montage of frames from a brightfield movie of the traps' being turned off and then back on as the sample containing the 2-μm beads is translated at 10 μm/s. The time between each successive frame is 1.0 s, as is indicated on the montage. At 0.0 s, six beads are shown in the traps. Then the traps are turned off momentarily to release the beads, which begin to move with the sample. New beads, however, are trapped. At times 2.0 and 3.0 s, there are two beads in the traps. At times 4.0 and 5.0 s, there are three beads in the traps. The objective was a 40×/0.65 NA Zeiss Achroplan oil objective. The arrow in each frame indicates the position of the row of traps.

of a laser beam to hold an object [16]. To hold multiple objects, a single focus typically is rapidly moved from one object to the next [17]–[19], while another straightforward means of trapping multiple particles is to use multiple beams and separately control the position of each focus [20], [21]. The multifocal microscope used in this work offers another means of trapping multiple particles. The size of the trapped particles would affect the allowed spacing between the foci since the optical forces on the particle depend strongly on the size of the particle and since traps spaced closer together than the particle size could both apply forces to the particle. Using a large number of closely spaced foci, however, which could be turned on or off separately, it should be possible to trap multiple particles and even to move particles simply by turning adjacent traps on or off. Working toward this end, we have demonstrated that multiple particles may be held in a multifocal microscope.

Fig. 10 shows a montage of frames from a brightfield microscopy movie of 2-μm polystyrene beads being held in the foci of four beamlets as the sample is translated at 10 μm/s. The objective used was a 40×/0.65NA Zeiss Achroplan air objective. With this objective, the spacing between the beamlets is $\sim$3.3 μm. The time between each successive frame is 1.0 s, as is indicated on the montage. One bead is held in each of four foci near the center of the frame as the other beads flow down with respect to the images. To highlight the motion of the other beads, we have used a white arrow in each frame to indicate the position of one of the flowing beads. Note that this bead is slightly out of the focal plane and hence appears to be larger in the images. Simple switching on and off of the multiple traps is shown in Fig. 11. The figure shows a montage of frames from a brightfield movie of the traps' being turned off and then back on as the sample containing the 2-μm beads is translated at 10 μm/s. The time between each successive frame is 1.0 s, as is indicated on the montage. At 0.0 s, six beads are shown in the traps. Then the traps are turned off momentarily to release the beads, which begin to move with the sample. New beads, however, are trapped after the traps are turned back on. At times 2.0 and 3.0 s, there are two beads in the traps. At times 4.0 and 5.0 s, there are three beads in the traps.

In the future, it should be possible to construct a microscope containing tens to hundreds of closely spaced foci with a switching element such as a micromachined micromirror array controlling each trap. In such a device, it should be possible to hold or to transport beads to any point in the array, simply by turning on or off the appropriate foci.

V. Summary

We have developed a high-efficiency temporally decorrelated array for multifocal multiphoton microscopy and multifocal micromachining that can take advantage of the high-average power of modern ultrashort-pulse lasers. The cascaded beamsplitter design allows efficient use of all the available light with the resolution of a single-focus multiphoton microscope. By increasing the number of foci, it will be possible to use high average power lasers to illuminate large areas of samples simultaneously instead of attenuating the beam and throwing away the majority of the available photons, as is currently done in most multiphoton microscopes. We have used this temporally decorrelated multifocal array to produce a multifocal microscope with which we have demonstrated multiphoton imaging using two-photon fluorescence, multifocal micromachining of optical waveguides, and multifocal optical trapping.

Acknowledgment

The authors gratefully acknowledge that none of this work would have been possible without the initial interest and financial support of Prof. K. R. Wilson.

References

[1] J. Bewersdorf, R. Pick, and S. W. Hell, "Multifocal multiphoton microscopy," *Opt. Lett.*, vol. 23, pp. 655–657, 1998.
[2] A. H. Buist, M. Muller, J. Squier, and G. J. Brakenhoff, "Real time two-photon absorption microscopy using multi point excitation," *J. Microsc.*, vol. 192, pp. 217–226, 1998.
[3] K. Fujita, O. Nakamura, T. Kaneko, M. Oyamada, T. Takamatsu, and S. Kawata, "Confocal multipoint multiphoton excitation microscope with microlens and pinhole arrays," *Opt. Commun.*, vol. 174, pp. 7–12, 2000.
[4] D. N. Fittinghoff and J. A. Squier, "Time-decorrelated multifocal array for multiphoton microscopy and micromachining," *Opt. Lett.*, vol. 25, pp. 1213–1215, 2000.
[5] D. N. Fittinghoff, P. W. Wiseman, and J. A. Squier, "Widefield multiphoton and temporally decorrelated multifocal multiphoton microscopy," *Opt. Express*, vol. 7, pp. 273–279, 2000.
[6] A. Egner and S. W. Hell, "Time multiplexing and parallelization in multifocal multiphoton microscopy," *J. Opt. Soc. Amer. A*, vol. 17, pp. 1192–1201, 2000.
[7] K. Konig, P. T. C. So, W. W. Mantulin, and E. Gratton, "Cellular response to near-infrared femtosecond laser pulses in two-photon microscopes," *Opt. Lett.*, vol. 122, pp. 135–136, 1997.

[8] A. E. Siegman, M. W. Sasnett, and T. F. Johnston, Jr., "Choice of clip levels for beam width measurements using knife-edge techniques," *IEEE J. Quantum Electron.*, vol. 27, pp. 1098–1104, 1991.
[9] P. W. Milonni and J. H. Eberly, *Lasers*. New York: Wiley, 1988.
[10] H. Dobson, "Pollen and pollen-coat lipids: Chemical survey and role in pollen selection by solitary bees (Pollenkitt, Oligolecty)," University of California, Berkeley, CA, 1985.
[11] K. M. Davis, K. Miura, N. Sugimoto, and K. Hirao, "Writing waveguides in glass with a femtosecond laser," *Opt. Lett.*, vol. 21, pp. 1729–1731, 1996.
[12] K. Miura, Q. Jianrong, H. Inouye, T. Mitsuyu, and K. Hirao, "Photowritten optical waveguides in various glasses with ultrashort pulse laser," *Appl. Phys. Lett.*, vol. 71, pp. 3329–3331, 1997.
[13] D. Homoelle, S. Wielandy, A. L. Gaeta, N. F. Borrelli, and C. Smith, "Infrared photosensitivity in silica glasses exposed to femtosecond laser pulses," *Opt. Lett.*, vol. 24, pp. 1311–1313, 1999.
[14] C. B. Schaffer, A. Brodeur, J. F. García, and E. Mazur, "Micromachining bulk glass by use of femtosecond laser pulses with nanojoule energy," *Opt. Lett.*, vol. 26, pp. 93–95, 2001.
[15] S. H. Cho, B. E. Bouma, E. P. Ippen, and J. G. Fujimoto, "Low-repetition-rate high-peak-power Kerr-lens mode-locked $Ti:Al_2O_3$ laser with a multiple-pass cavity," *Opt. Lett.*, vol. 24, pp. 417–419, 1999.
[16] A. Ashkin, J. M. Dziedzic, J. E. Bjorkholm, and S. Chu, "Observation of a single-beam gradient force optical trap for dielectric particles," *Opt. Lett.*, vol. 11, pp. 288–290, 1986.
[17] K. Visscher, G. J. Brakenhoff, and J. J. Krol, "Micromanipulation by 'multiple' optical traps created by a single fast scanning trap integrated with the bilateral confocal scanning laser microscope," *Cytometry*, vol. 14, pp. 105–114, 1993.
[18] C. Mio, T. Gong, A. Terray, and D. W. M. Marr, "Design of a scanning laser optical trap for multiparticle manipulation," *Rev. Sci. Instrum.*, vol. 71, pp. 2196–2200, 2000.
[19] H. Misawa and S. Juodkazis, "Photophysics and photochemistry of a laser manipulated microparticle," *Progress Polymer Sci.*, vol. 24, pp. 665–697, 1999.
[20] K. Visscher, S. P. Gross, and S. M. Block, "Construction of multiple-beam optical traps with nanometer-resolution position sensing," *IEEE J. Select. Topics Quantum Electron.*, vol. 2, pp. 1066–1076, 1996.
[21] E. Fallman and O. Axner, "Design for fully steerable dual-trap optical tweezers," *Appl. Opt.*, vol. 36, pp. 2107–2113, 1997.

David N. Fittinghoff received the B.S. degree in physics from the University of California, Davis, in 1985 and the M.S. and Ph.D. degrees in engineering applied science from the University of California, Davis, in 1989 and 1993, respectively.

His research has covered strong-field ionization of atoms, ultrashort pulse measurement including frequency-resolved optical gating, multiphoton microscopy, and the development of chirped pulse amplification systems. He is currently a Researcher with the Institute for Nonlinear Science, University of California, San Diego.

Dr. Fittinghoff is a member of the Optical Society of America and the American Physical Society.

Chris B. Schaffer received the undergraduate degree from the University of Florida, Gainesville, in 1995 and the Ph.D. degree from Harvard University, Cambridge, MA, in 2001, both in physics.

He is currently a Postdoctoral Research Associate at the University of California, San Diego. His research interests include using femtosecond laser pulses for nonlinear microscopy and micromachining and investigating the fundamental interaction mechanisms between femtosecond laser pulses and materials.

Eric Mazur received the Ph.D. degree in experimental physics from the University of Leiden, The Netherlands.

He is a Professor at Harvard College, Gordon McKay Professor of Applied Physics, and Professor of physics at Harvard University. He leads a vigorous research program in optical physics, emphasizing spectroscopy, light scattering, and studies of electronic and structural events in solids that occur on the femtosecond time scale. In 1984, he joined the Faculty of Harvard University and obtained tenure six years later. In addition to his work in optical physics. Dr. Mazur is interested in education, science policy, outreach, and the public perception of science. He has served on numerous committees and councils, including advisory and visiting committees for the National Science Foundation; has chaired and organized national and international scientific conferences; and has presented to the Presidential Committee of Advisors on Science and Technology. He is a Consultant to industry in the electronics and telecommunications industry. He is author or coauthor of more than 120 scientific publications. He is the author of *Peer Instruction: A User's Manual* (Englewood Cliffs, NJ: Prentice-Hall, 1997), which explains how to teach large lecture classes interactively.

Dr. Mazur is a fellow of the American Physical Society. In 1988, he received a Presidential Young Investor Award. He has been named APS Centennial Lecturer during the society's centennial year.

J. A. Squier received the B.S. and M.S. degrees from the Colorado School of Mines, Golden, and the Ph.D. degree from the Institute of Optics, University of Rochester, Rochester, NY.

His disseration topic was ultrafast solid-state lasers. His present interests include the application of ultrafast lasers to microscopy, quantum control, the generation of ultrafast X-rays, and medical imaging. He will be joining the Physics Department, Colorado School of Mines, in fall 2002.

Dr. Squier is a Fellow of the Optical Society of America.